Genetic population structure and demographic history of the sailfin sandfish *Arctoscopus japonicus* associated with sea level changes during the Last Glacial Maximum

Hiroaki Kurihara[1],*, Minoru Ikeda[1,2]

[1]Laboratory of Marine & Coastal Ecosystem Science, Onagawa Field Center, Graduate School of Agriculture, Tohoku University, 2-10-1, Konori, Onagawa, Oshika, Miyagi 986-2248, Japan
[2]Tohoku University & JAMSTEC Advanced Institute for Marine Ecosystem Change (WPI-AIMEC), 6-3 Aoba, Aramaki, Aoba-ku, Sendai 980-8578, Japan

ABSTRACT: Understanding the genetic population structure and demographic history of a fishery resource species is important for resource management that considers the viability and evolutionary potential of the species. The sailfin sandfish *Arctoscopus japonicus* is an important resource in Japan. Its population structure has been investigated in previous studies, but a mismatch between morphometric and population genetic analysis was observed. We investigated whether this mismatch could be attributed to the detection sensitivity of DNA markers by analyzing nuclear microsatellite loci. We also estimated the formation process of the population structure through demographic analysis based on mitochondrial DNA. Our analysis revealed the presence of formerly undetected subtle genetic differences between local populations, which were consistent with the findings of the previous morphometric study. Demographic analysis suggests that the most diverged populations of the Pacific Ocean and Sea of Japan differentiated as a result of vicariance during the last glacial period. We also found that the Sea of Okhotsk population may have originated from admixture between Pacific Ocean and Sea of Japan individuals. These results provide new insights into the population structure of the species, which are essential for resource management.

KEY WORDS: Phylogeography · Historical demography · Nucleotide substitution rate · Approximate Bayesian computation · Management unit

1. INTRODUCTION

The sailfin sandfish *Arctoscopus japonicus* is a benthopelagic fish distributed in the Sea of Japan, the Pacific Japanese coast from northeastern Honshu (i.e. mainland of Japan) to Hokkaido, and the Sea of Okhotsk (Okiyama 1970, 1990, Mecklenburg 2003). It is an important fishery resource in Japan, caught in bottom-trawl and fixed-net fisheries with annual catches of several thousand tonnes (Fujiwara et al. 2020, Iida et al. 2020). Fisheries management

of wild marine resources is typically conducted at the level of stocks with independent population demography. Stock delineation based on the genetic population structure of a species can support resource management that considers the viability and evolutionary potential of the species (Moritz 1994, Palsbøll et al. 2007). Furthermore, inferring not only the population structure but also the process of its formation can provide insights for predicting the response of the species to future climate change by revealing the relationship between historical pop-

ulation demography and environmental change (Hotaling et al. 2018).

In previous studies, the genetic population structure of *A. japonicus* has been investigated through analyses of allozymes (Fujino & Amita 1984) and mitochondrial DNA (mtDNA) (Yanagimoto 2004, Shirai et al. 2006). In their analyses based on the mtDNA control region, Yanagimoto (2004) and Shirai et al. (2006) demonstrated significant genetic differentiation between local populations in the Sea of Japan and Pacific Ocean. In addition, Shirai et al. (2006) showed that there are 2 deeply divergent mtDNA haplogroups (Haplogroups A and C; B is endemic to the Pacific Ocean) within the Sea of Japan. They identified the presence of 2 genetic groups in this sea area distinguished by differences in their haplotype frequency. They concluded that this species is composed of at least 3 genetic groups (Southern Hokkaido, SH; West coast of Japan, WJ; and East coast of Korea, EK). However, it has been shown that some spawning schools within these genetic groups can be distinguished by differences in their morphometric characters (Okiyama 1970, Kobayashi & Kaga 1981), and it has also been suggested that they may have different migration ranges (Yanagimoto & Konishi 2004). Therefore, it is possible that there is a fine-scale population structure within the genetic groups recognized by Shirai et al. (2006), which has potential to impact fisheries management, although the previous population genetic study found no evidence to support this (Fujino & Amita 1984, Yanagimoto 2004, Shirai et al. 2006). To examine whether fine-scale genetic differences exist between local populations, it is necessary to analyze more polymorphism-rich and fast-evolving nuclear DNA markers such as microsatellite DNA (msDNA) loci (Guichoux et al. 2011), which has not been done for this species so far.

In the present study, we aimed to examine the genetic population structure of *A. japonicus* using msDNA analysis. We also conducted demographic analysis based on the mtDNA cytochrome *b* (cyt*b*) region to investigate the relationship between past climate change events and the establishment process of the population structure of this species. (1) We estimated the genetic population structure based on genetic data from both msDNA and the mtDNA cyt*b* sequence. To assess the reliability of the detected genetic population structure, we conducted multiple different analyses and compared the results. (2) To reconstruct the historical population demography, we estimated the molecular evolutionary rate of mtDNA in *A. japonicus*. This involved estimating the divergence time within the perciform suborder Cottoidei

(Nelson et al. 2016), to which *A. japonicus* is classified, utilizing complete mitochondrial gene sequences and fossil records. (3) We conducted a population demographic analysis based on the mtDNA cyt*b* sequence using the estimated molecular evolutionary rates. Here, we particularly highlight geological epochs after the Last Glacial Maximum (LGM, ca. 20 thousand years ago [kya]), which is thought to have greatly influenced the shaping of the population structure of present-day wild organisms (Avise 2000), and assess the profound impact of rapid climate fluctuations on the population demographic history of this species. Specifically, incorporating results from population structure analyses, we enumerated and compared several plausible demographic scenarios associated with climatic events. Based on the inferred population demographic history, we attempted to reconstruct the relationship between the formation of the population structure and past climate change.

2. MATERIALS AND METHODS

2.1. Sample collection and laboratory procedures

The specimens of sailfin sandfish *Arctoscopus japonicus* used in this study were sampled across its distribution around the Japanese archipelago (Fig. 1, Table 1). We analyzed 240 extracted DNA samples (about 10 ng μl⁻¹) from the same 8 sites (Akkeshi, Muroran, Atsuta, Hachimori, Funagawa, Wakasa, Oki, and Mishima) along the coast of Honshu used by Shirai et al. (2006), and 30 new samples collected in October 2004 from the Sea of Okhotsk coast of Hokkaido (Abashiri). Genomic DNA from the newly added specimens (tissue slices stored in 99.5% ethanol) was extracted using DNeasy Blood & Tissue Kits (Qiagen) following the manufacture's handbook. In Shirai et al. (2006), the sample populations were assigned to the following 3 geographic groups: Akkeshi and Muroran to the SH group; Atsuta, Hachimori, Funagawa, Wakasa, and Oki to the WJ group, and Mishima to the EK group (Fig. 1, Table 1).

2.2. Sequencing of the cyt*b* region

For the mtDNA cyt*b* region, PCR and sequencing primers were designed based on the *A. japonicus* mitochondrial genome sequence (GenBank accession number: AP003090). The primer L-Glu14345.Aj (5'-AAC CAC CGT TGT AAC TCA ACT AC-3') was located upstream of the target region in the tRNA^Glu re-
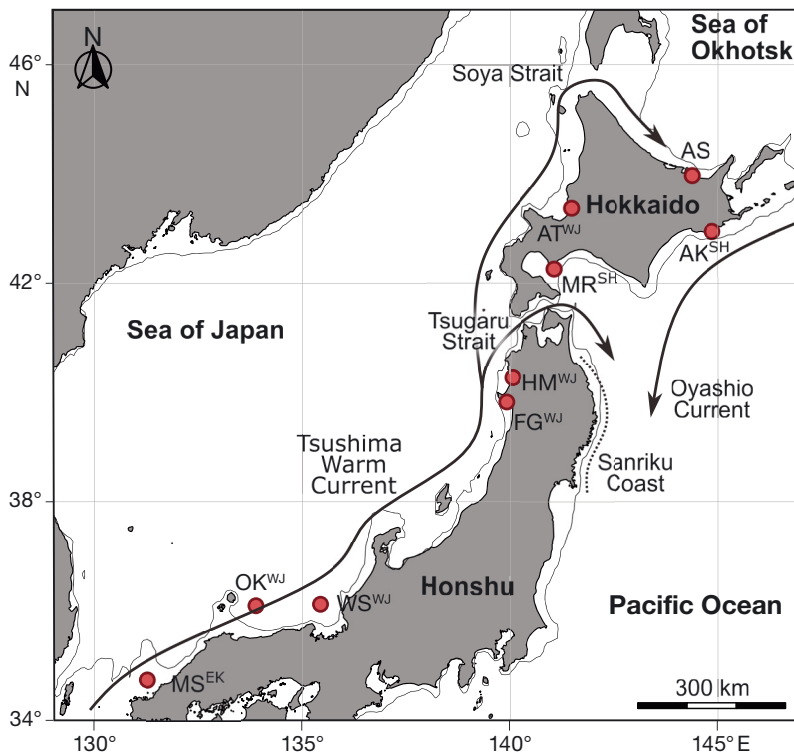
Fig. 1. Sampling locations (red dots). The abbreviations for each sample population are as follows: AS: Abashiri (Abashiri stock); AT: Atsuta (Ishikari Bay stock); AK: Akkeshi (Kushiro stock); MR: Muroran (Funka Bay stock); HM: Hachimori and FG: Funagawa (Northern Sea of Japan stock); WS: Wakasa, OK: Oki, and MS: Mishima (Western Sea of Japan stock). The superscript letters next to the abbreviations for each location indicate the 3 genetic groups (SH: Southern Hokkaido; WJ: West coast of Japan; EK: East coast of Korea) to which each sample population belongs, according to Shirai et al. (2006). The coastline during the Last Glacial Maximum (LGM) (depth of 130 m) is indicated (solid line)

Table 1. Collections of *Arctoscopus japonicus* samples for the present study. na: not applicable; genetic-group abbreviations as in Fig. 1

Sampling sites (code)	Date sampled	Sample size	Genetic group by Shirai et al. (2006)	GenBank accession no.
Sea of Okhotsk				
Abashiri (AS)	Oct 2004	30	na	LC787018−LC787046
Pacific Ocean				
Akkeshi[a] (AK)	May 2000	30	SH	LC786958−LC786987
Muroran[a] (MR)	Nov 1999	30	SH	LC786988−LC787017
Sea of Japan				
Atsuta[a] (AT)	Nov 1999	30	WJ	LC787047−LC787076
Hachimori[a] (HM)	Dec 1999	30	WJ	LC787077−LC787106
Funagawa[a] (FG)	Dec 1999	30	WJ	LC787107−LC787134
Wakasa[a] (WS)	Jul 2000	30	WJ	LC787135−LC787164
Oki[a] (OK)	Mar 2000	30	WJ	LC787165−LC787194
Mishima[a] (MS)	Mar 2000	30	EK	LC787195−LC787224

[a]Samples identical to those used by Shirai et al. (2006)

gion, and the primer H-Pro15610.Aj (5′-TTG GGG GTT AGG GGT GGG AGT T-3′) was located downstream in the tRNA[Pro] region. The PCR mixture for the partial the cyt*b* sequence was as follows: Blend Taq® Plus (0.125 µl) (TOYOBO), 10× PCR Buffer for Blend Taq (1.25 µl), 2mM dNTPs (1.25 µl), 100 pmol µl^{-1} of each primer (0.125 µl), ultra-purified water (9.125 µl), and extracted DNA (1 µl) in a reaction volume of 13 µl. The PCR conditions included an initial denaturation at 94°C for 2 min, and 28 cycles of denaturation at 94°C for 30 s, annealing at 58°C for 30 s, and extension at 72°C for 1 min. PCR products were purified with Agencourt AMPure XP (Beckman Coulter) and diluted in 40 µl of ultra-purified water. Purified products were sequenced using the primers listed above with the BigDye Terminators v3.1 Cycle Sequencing Kit (Applied Biosystems), according to the manufacturer's instructions, and visualized on a 3500 XL Genetic Analyzer (Thermo Fisher Scientific). Finally, we used ATGC ver. 7.03 (GENETYX) to assemble the sequence of the target region from the L and H chains. For each sample population, we calculated the number of haplotypes, haplotype diversity (*h*), and nucleotide diversity (π) using Arlequin ver. 3.5.2.2 (Excoffier & Lischer 2010) for each site sampled.

2.3. Genotyping of the microsatellite DNA loci

We selected 10 microsatellite loci (*DR225*, *DR148*, *DR5*, *Orla16-32*, *Orla17-188*, *Orla2-91*, *Orla21-231*, *Orla3-65*, *Orla5-131*, and *Orla9-204*) based on the following criteria established in a previous study (Kurihara & Ikeda 2022): absence of null alleles and large allele dropout, and no deviation from Hardy-Weinberg equilibrium (HWE) proportions within each sample population as expected in a panmictic population. Fragment analysis was conducted using the method described by Blacket et al. (2012), following Strategy II: Singleplex

using multiple fluorophores. The PCR mixture for microsatellite fragment analysis was as follows: Tks Gflex DNA Polymerase (0.2 µl) (TaKaRa Bio), 2× Gflex PCR Buffer (5.0 µl), 5 pmol µl^{-1} forward primer with tail sequence (0.3 µl), 5 pmol µl^{-1} reverse primer (1.0 µl), 5 pmol µl^{-1} universal primer with fluorescent tag (0.4 µl), ultra-purified water (2.3 µl), and extracted DNA (1 µl) in a reaction volume of 6 µl. The PCR mixture was used as the template for the microsatellite fragment analysis. The PCR conditions followed those of Kurihara & Ikeda (2022). The PCR products and GeneScan 600 LIZ size standard (Applied Biosystems) were loaded onto an automated DNA sequencer (SeqStudio Genetic Analyzer, Thermo Fisher Scientific) and fragment analysis was conducted by capillary electrophoresis. The size of each allele was determined using GeneMapper ver. 6.0 (Applied Biosystems). For each sample population, we calculated the number of alleles (n_a), the effective number of alleles (n_e; Kimura & Crow 1964), the mean expected heterozygosity (H_e), and the mean observed heterozygosity (H_o), using GenAlEx ver. 6.5 (Peakall & Smouse 2012).

2.4. Genetic population structure analysis based on the cyt*b* sequences

To elucidate the phylogenetic relationships among the haplotypes, phylogenetic analysis was performed. *Trichodon trichodon* (GenBank accession number LC125776), a sister species of *A. japonicus*, was used as an outgroup. The DNA haplotypes were aligned using MAFFT ver. 7.453 (Katoh & Standley 2013) and trimmed to a length of 612 bp to match the sequence of LC125776. The nucleotide substitution model was selected based on the Bayesian information criterion (BIC) using MEGA7 (Kumar et al. 2016). Tree topology was estimated using the neighbor-joining method with 1000 bootstrap replications implemented in MEGA7 and the Bayesian method implemented in BEAST ver. 2.6.6 (Bouckaert et al. 2014). In the BEAST analysis, the coalescent Bayesian skyline model was assumed as the tree prior. For the Markov chain Monte Carlo (MCMC) analysis, the parameters were sampled every 10000 steps to obtain 1.0×10^8 records after discarding the first 1.0×10^7 records as burn-in. The effective sample size (ESS) was confirmed to be >200 using Tracer ver. 1.7.1 (Rambaut et al. 2018).

The genetic population structure of *A. japonicus* was estimated using a clustering analysis based on the mtDNA sequence. We performed SAMOVA ver. 2.0 (spatial analysis of molecular variance; Dupanloup et al. 2002) with 10000 permutations, which as-

sumed that the number of clusters (K) is between 2 and 6. SAMOVA is a method of clustering sample populations by considering geographic locations, such that the genetic variance between clusters (Φ_{CT} and V_a) is maximized for any given number of clusters K. The optimal value for K was determined by adopting the minimum K at which $V_b = 0$ (genetic variance between sample populations within the cluster) and was statistically supported based on the parsimony criterion ($\alpha = 0.05$). Pairwise Φ_{ST} between the clusters detected by the above analysis was evaluated using 10000 permutations in Arlequin ($\alpha = 0.05$). A sequential Bonferroni correction for multiple tests (Rice 1989) was applied.

2.5. Genetic population structure analysis based on microsatellite DNA variations

Cluster analysis was performed based on msDNA data. First, Nei's standard genetic distance, D_S (Nei 1972), matrix was calculated using POPULATIONS (https://bioinformatics.org/populations/), and a population-based neighbor-joining tree (Saitou & Nei 1987) was constructed based on this matrix, with 1000 bootstrap analyses. Additionally, a neighbor-net (Bryant & Moulton 2004) was constructed using SplitsTree4 (Huson & Bryant 2006) based on the distance matrix.

Discriminant analysis of principal components (DAPC) was performed using the R package adegenet (Jombart et al. 2010) to clarify the genetic relationships among the sample populations. DAPC was conducted for 2 datasets: one including all 9 sample populations (ALL), and one including only the sample populations from the Sea of Japan (SJ: Atsuta, Hachimori, Funagawa, Wakasa, Oki, and Mishima). The optimal number of principal components was determined based on the results of 100 cross-validations (90% for training and 10% for validation; ALL: 69; SJ: 74). The number of discriminant axes was set to 8 for the ALL dataset and 5 for the SJ dataset.

PopCluster ver. 1.1.0.0 (Wang 2022) was used to estimate the individual assignment to each of K clusters using both model-based (admixture model) and non-model-based (k-means) methods. We conducted the analysis for 2 datasets: Dataset ALL and a dataset containing only samples from the Pacific coast of Hokkaido (PO: Akkeshi and Muroran). For the analysis assuming the admixture model, we set the scaling parameter to 0 and applied the unequal allele frequency prior. For each K, we assumed $K = 1-10$ for the ALL dataset and $K = 1-4$ for the PO dataset, and calculated D_{LK2} values and mean F_{STIS}

values by performing 10 independent analyses. D_{LK2} values reflect the changes in log-likelihood with K, while mean F_{STIS} values measure population differentiation and the deviation from HWE within clusters. Based on these two values, we determined the optimal K. Pairwise F_{ST} and R_{ST} between the clusters detected by the above analysis and AMOVA was evaluated using 10 000 permutations in Arlequin (α = 0.05). A sequential Bonferroni correction for multiple tests was applied.

2.6. Calibration of the molecular evolutionary rate for the cyt*b* region

To reconstruct the demographic history of *A. japonicus* based on DNA sequence data, we first estimated the molecular evolutionary rate of the mtDNA cyt*b* region with the Cottoidei time-calibrated tree based on mitochondrial genome datasets. The phylogenetic tree topology of the Cottoidei species was estimated based on the maximum likelihood method (Felsenstein 1981) using RAxML ver. 8.2.12 (Stamatakis 2014). The 7 ingroup and 1 outgroup species were selected following Imamura et al. (2005) and Nelson et al. (2016) (Table S1 in the Supplement at www.int-res.com/articles/suppl/m747p133_supp.pdf). We used 12 protein-coding gene regions, excluding the ND6 gene region, from the complete mitochondrial genome sequences obtained from GenBank. The ND6 region was excluded from the phylogenetic analyses due to its inconsistent phylogenetic performance and heterogeneous base composition (Zardoya & Meyer 1996, Miya & Nishida 2000). The remaining 12 protein-coding gene DNA sequences were aligned using MAFFT. From the aligned sequence matrix, we trimmed the start and stop codon regions and overlapping regions between genes. The trimmed sequences were concatenated using the fasconcat.pl program (Kück & Meusemann 2010). We performed a tree topology search using the rapid bootstrap algorithm (-f a option) implemented in RAxML with 1000 bootstrap replicates under the GTR+Γ model (Yang 1994, the model recommended by the author of the program). To examine whether the dataset and data partitioning conditions influence the inferred tree topology, 6 distinct configurations were analyzed by applying 2 partitioning schemes to the data matrices. The first scheme involved dividing the data based on gene regions, while the second scheme treated the entire data matrix as a single unit. These partitioning schemes were applied to 3 variants of the data matrix: (1) full-length sequences containing all codon positions $(1_N2_N3_N)$, (2) sequences excluding the third codon positions due to their fast substitution rates (1_N2_N), and (3) sequences with the third codon positions encoded as purines and pyrimidines using RY encoding $(1_N2_N3_{RY})$. In the above analysis, it was assumed that each partition had different branch lengths (-M option: implemented in RAxML).

To estimate the molecular evolutionary rates of mitochondrial genome genes in the Cottoidei, MCMCTREE in the PAML 4.9h package (Yang 2007) was used to time-calibrate the phylogenetic tree obtained. The dataset was partitioned into coding regions and the molecular evolutionary rate for each region was estimated. The fossil records used to calibrate the divergence times are shown in Table S2. The MCMCTREE analysis employed an approximate likelihood method (dos Reis & Yang 2011). The independent rates model (clock2) was applied to rate variation between branches, and the HKY+Γ model (Hasegawa et al. 1985) was assumed. The overall substitution rate (rgene gamma) and the rate-drift parameter (sigma2 gamma) were assigned Gamma distribution priors with shape parameter α and scale parameter β: G(α, β), using the method described by Inoue et al. (2010), where G(1, 43) and G(1, 49) were applied, respectively. For the MCMC analysis, the parameters were sampled every 2 steps to obtain 1.0×10^5 records after discarding the first 1.0×10^4 records as burn-in. ESS was confirmed to be greater than 200 using Tracer. The analysis was run twice, and convergence of the Markov chains was assessed by comparing the estimated values.

2.7. Reconstruction of demographic history

We reconstructed historical demography based on the mtDNA dataset to investigate the association between climate change events during the ice age cycles of the Pleistocene and the establishment of the group structure of *A. japonicus* in the Sea of Japan and the Pacific. Hachimori, Funagawa (representing the WJ group in the Sea of Japan, Shirai et al. 2006), and Akkeshi (representing the SH group in the Pacific Ocean) were selected for this analysis (Fig. 1, Table 1).

The assumption of population equilibrium and selective neutrality was tested with Tajima's D (Tajima 1989) and Fu's F_S (Fu 1997) statistics through 1000 simulations in Arlequin. Next, a demographic scenario was selected based on the approximate Bayesian computation (ABC) framework as implemented in DIYABC ver. 2.1.0 (Cornuet et al. 2014). For comparison, 6 scenarios were constructed considering the divergence

time between the WJ and SH groups, the presence or absence of secondary contact, and the presence or absence of population expansion of the WJ group (Fig. 2): (1) the SH group diverged from the WJ group after the LGM, at $t_0 < 19\,000$ yr ago; (2) the SH group diverged from the WJ group before the LGM, at $t_2 > 21\,000$ yr ago; (3) after the LGM, the SH group diverged from the WJ group (at t_0) and the distribution of the WJ group expanded at t_1 ($t_0 < t_1$); (4) before the LGM, the SH group diverged from the WJ group (at t_2), and after the LGM the WJ group expanded (at t_1); (5) before the LGM, the SH group diverged from the WJ group (at t_2) and both groups had secondary contact after the LGM (at t_0); (6) before the LGM, the SH group diverged from the WJ group (at t_2), and after the LGM, the WJ group expanded (at t_1), then both groups had secondary contact (at t_0). We assumed a uniform prior distribution for the per-site, per-generation mean substitution rate of the mtDNA cyt*b* region with an upper and lower bound on the 95 % highest posterior probability density (HPD) interval estimated using the method described above (Section 2.6).

A. japonicus is considered to mature in 2 to 3 yr (Kiyokawa 1991) and thus, following Shirai et al. (2006), we assumed that the generation time of this species is 2.5 yr. Prior distributions for effective population sizes, divergence times, and admixture proportions are summarized in Table S3. For each scenario,

1.0×10^5 coalescent simulations were performed, and the following summary statistics were calculated for every simulation: the number of haplotypes, number of segregating sites, mean pairwise difference, variance of pairwise differences, Tajima's D, private segregating sites, mean number of the rarest nucleotide at segregating sites, variance of the number of the rarest nucleotide at segregating sites, and pairwise F_{ST}. After simulations, the posterior probabilities for each scenario were compared using a logistic approach: logistic regression with linear discriminant analysis was used to estimate the posterior probabilities based on the summary statistics. This was achieved by utilizing 0.1 to 1 % of the simulated data exhibiting the highest degree of similarity to the observed data. Principal component analysis (PCA) was performed to confirm whether or not the observed values of summary statistics can be simulated under the best scenario.

Finally, we performed a coalescent-based analysis using MIGRATE ver. 3.7.1 (Beerli 2006) to estimate the change in population size and migration rate through time. Posterior probabilities of the parameters were searched by MCMC algorithm. The parameters were sampled every 100 steps to obtain 1.0×10^8 records after discarding the first 1.0×10^5 records as burn-in. We employed a static heating scheme using 4 chains with different temperatures (temperature of each chain: 1.0×10^6, 3.0, 1.5, 1.0) to avoid entrapment in local optima. After running the MCMC, we confirmed, using Tracer, that the ESS was $\geqslant 200$. The estimated mutation-scaled parameters were converted to female effective population size (fN_e), female migration rate (m), and calendar date (t), assuming the substitution rate which was the estimated median rate as described above (Section 2.6).
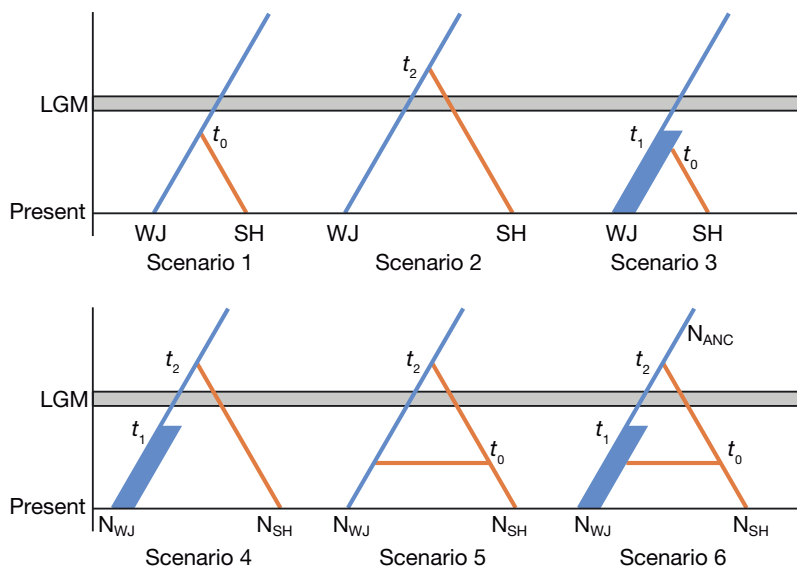

Fig. 2. Six demographic scenarios (see Section 2.7) examined using approximate Bayesian computation (ABC) based on mitochondrial DNA sequences. The histories of different populations are represented by colored lines (blue: Sea of Japan population, WJ; orange: Pacific population, SH), with line bifurcations indicating population splits, and line mergers indicating secondary contact after population splitting. Changes in line thickness represent changes in population size. Associated characters (t_0, t_1 and t_2) in each diagram are model parameters described in the text (Section 2.7) and Table S3. LGM: Last Glacial Maximum

3. RESULTS

3.1. Genetic population structure analysis based on mitochondrial DNA variations

The contiguity of the 1136 bp sequences was determined by combining partial DNA sequences from the cyt*b* (bases 59 to 1141) and tRNA^{Thr} (bases 1 to 53) regions. This dataset consists of a total of 155 haplotypes defined by 155 variable sites (Table S4). The TN93+Γ (Tamura & Nei 1993)
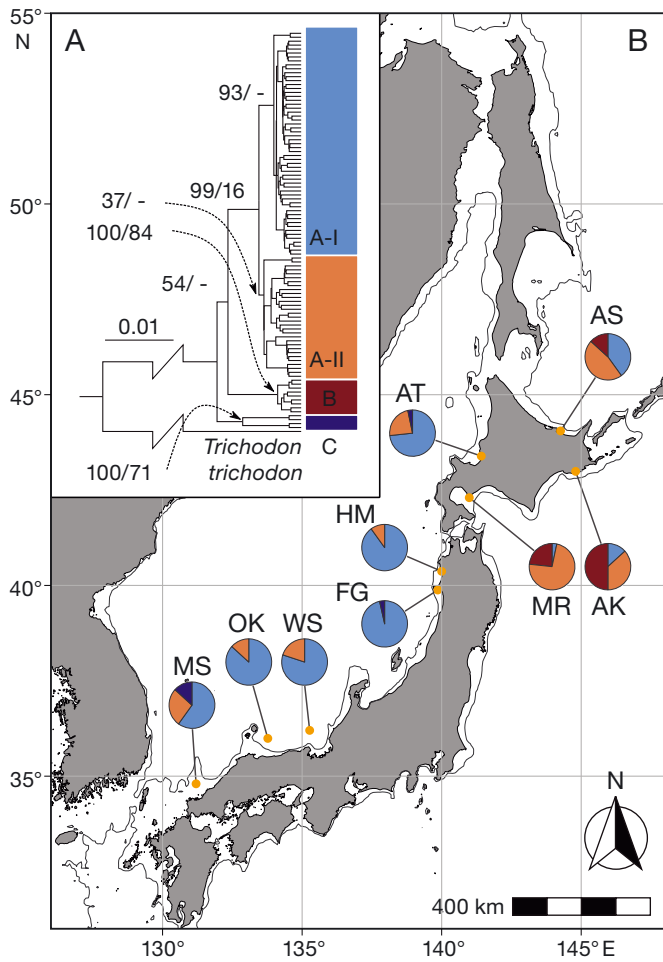
Fig. 3. (A) Phylogenetic relationships of mitochondrial DNA haplotypes constructed using Bayesian inference and (B) geographical distribution of each haplogroup. The numbers on internal nodes in the phylogenetic tree represent Bayesian posterior probabilities and bootstrap values (neighbor-joining tree), and the colors of the clades and pie charts correspond to each other. The coastline during the Last Glacial Maximum (LGM) (depth of 130 m) is indicated (solid line). See Table 1 for sample population abbreviations

model was selected based on the BIC. The phylogenetic analysis revealed 3 clades (A, B, and C) with posterior probabilities ranging from 99 to 100% (Fig. 3A). Although the bootstrap values were low, these clades were also reconstructed by the neighbor-joining method (bootstrap support: 16 to 71%). For Clade A in the Bayesian tree, however, a subclade consisting of A-I and A-II was reconstructed with low posterior probabilities (A-I: 93%; A-II: 37%).

Among the sample populations, haplogroup frequencies belonging to each clade varied, and regional differences were observed (Fig. 3B). Haplotypes in Clade A were observed in all sample populations. Haplotypes in Clade B were observed only in sample populations from the Pacific Ocean and the Sea of Okhotsk, with a high frequency in the former (0.233 and 0.500 in Akkeshi and Muroran, respectively, and 0.133 in Abashiri). Clade C is genetically the most distant from the others, and its haplotypes were observed only in the Sea of Japan population, particularly at a high frequency in the Mishima population (haplogroup frequency 0.133). The presence of subclades within Clade A can be considered ambiguous from a statistical perspective, as it depends on the methodology used. However, there was a tendency for the haplotypes of Subclade A-I to be more frequent in the Sea of Japan population, while the haplotypes of Subclade A-II showed a higher frequency in the Pacific population.

Based on the SAMOVA clustering of mtDNA data, the minimum value of K (where statistically $V_a > 0$ and $V_b = 0$) indicated that the best assumption is 5 clusters (Table 2, $V_a = 1.320$, $V_b = 0.007$). The Φ_{CT} value at the best K was 0.268, and 26.8% of the total genetic variation was explained by the genetic variation among clusters. In the SAMOVA at $K = 5$, the 5 samples from the Sea of Japan (Atsuta, Hachimori, Funagawa, Wakasa, and Oki) were grouped together into a single cluster which corresponds to the WJ group (Shirai

Table 2. SAMOVA clustering. **Bold**: Best hierarchical model (population structure) with the highest V_a/V_b value; parentheses: p-value. See Table 1 for sample population abbreviations. *Since V_b is negative, V_a/V_b is an invalid value and was not calculated

| Number of clusters | Hierarchical model | Variance component | | | Ratio of variance component V_a/V_b |
| | | Among groups (V_a) | Among locality | | |
			Within groups (V_b)	Within locality (V_c)	
2	(AK, MR),(AS,AT,HM,FG,WS,OK,MS)	1.834 (0.038)	0.243 (<0.001)	3.592 (<0.001)	7.540
3	(AK),(MR),(AS,AT,HM,FG,WS,OK,MS)	1.706 (0.023)	0.245 (<0.001)	3.592 (<0.001)	6.975
4	(AK),(MR),(AS),(AT,HM,FG,WS,OK,MS)	1.484 (0.017)	0.096 (0.002)	3.592 (<0.001)	15.437
5	**(AK),(MR),(AS),(AT,HM,FG,WS,OK),(MS)**	**1.320 (0.006)**	**0.007 (0.091)**	**3.592 (<0.001)**	**189.954**
6	(AK),(MR),(AS),(AT),(HM,FG,WS,OK),(MS)	1.178 (0.008)	−0.022 (0.276)	3.592 (<0.001)	*

et al. 2006; Fig. 1, Table 1), while the remaining samples (Akkeshi, Muroran, Abashiri, and Mishima) each formed distinct groups. Pairwise Φ_{ST} was calculated based on the results of this clustering, and all 5 detected clusters were significantly differentiated in all combinations (Table 3). The Φ_{ST} values were higher between the Sea of Japan and Pacific Ocean sample populations (Φ_{ST} = 0.218–0.463, p < 0.001) and lower within the groups for each sea area (Φ_{ST} = 0.048–0.077, p = 0.000–0.013).

3.2. Genetic population structure analysis based on microsatellite DNA variations

There was no null allele and large allele dropout, and HWE was confirmed for all populations. The mean number of alleles (n_a) in the sample population was 13.3 (SD = 1.128), the mean effective number of alleles (n_e) was 7.8 (SD = 0.600), and the H_o was 0.772 (SD = 0.0195; Table S4).

The population-based neighbor-joining tree showed a relatively large genetic differentiation between the Sea of Japan and the other sample populations (Fig. 4A). Within the Sea of Japan, 3 clusters (Atsuta; the Northern Sea of Japan, which includes the Hachimori and Funagawa populations; and the Western Sea of Japan, which includes the Wakasa, Oki and Mishima populations, Fig. 4C) were consistently supported by bootstrap values of 62 to 88%, although their internal branches were relatively short, indicating a low level of differentiation. Neighbor-net also explained the genetic differentiation between the Sea of Japan and the other sample populations and the 3 genetic clusters within the Sea of Japan (Fig. 4B), similar to the neighbor-joining tree. However, it showed notable network structures among all clusters except for those from the Northern Sea of Japan and the

Table 3. Genetic divergence among the 5 clusters suggested by SAMOVA clustering. Below diagonal: pairwise Φ_{ST}; above diagonal: p-values. Statistical significance was tested by permutation tests (10 000 permutations), and p-values were corrected by sequential Bonferroni. WJ: West coast of Japan, which includes Hachimori, Funagawa, Wakasa, and Oki samples

Clusters	Akkeshi	Muroran	Abashiri	WJ	Mishima
Akkeshi		<0.001	<0.001	<0.001	<0.001
Muroran	0.05223		<0.001	<0.001	<0.001
Abashiri	0.15351	0.09082		<0.001	<0.001
WJ	0.46291	0.42667	0.17948		<0.001
Mishima	0.26281	0.2183	0.04801	0.07734	

Western Sea of Japan, suggesting gene flow between these clusters.

The results of DAPC were supported by the neighbor-joining tree and neighbor-net (Fig. 4D,E). For the ALL dataset, the first axis reflected the genetic differences between individuals from the Sea of Japan and those from the Pacific Ocean, with individuals from Abashiri in the Sea of Okhotsk situated in between. The second axis mainly reflected the genetic differences within each sea area (Fig. 4D). On this axis, individuals from the Akkeshi and Muroran populations in the Pacific Ocean were clearly differentiated from each other. For the SJ dataset, the DAPC results also suggested the presence of 3 groups: Atsuta, the Northern Sea of Japan, and the Western Sea of Japan (Fig. 4E). The first axis reflected the differences between the Northern Sea of Japan and the other populations, while the second axis represented geographic genetic differences among the north to south clusters within the Sea of Japan.

A population structure consistent with the population-based clustering analysis was also detected through individual-based clustering analysis using PopCluster. The analysis based on the ALL dataset showed that the D_{LK2} value was maximized at $K = 2$ and the F_{STIS} value was maximized at $K = 5$ (Fig. 5D). Based on the results of assignment by the admixture model and k-means clustering, each cluster at $K = 2$ was mainly associated with populations in the Sea of Japan and the Pacific Ocean (Fig. 5A). The Abashiri sample population in the Sea of Okhotsk had many individuals with characteristics of both clusters. When $K = 5$ (Fig. 5B), individuals from Akkeshi and Muroran in the Pacific Ocean (corresponding to the SH group, Shirai et al. 2006; Fig. 1, Table 1 in this article) were assigned to Cluster 1 with high probability. Individuals from Abashiri were primarily assigned to Cluster 2, with some belonging to Clusters 1, 3 or 4. Clusters 3, 4, and 5 primarily characterized individuals from the Sea of Japan. Specifically, individuals from Atsuta mainly belonged to Cluster 3. Cluster 4 was characteristically detected in the Northern Sea of Japan, including Hachimori and Funagawa, while Cluster 5 was predominantly found in the Western Sea of Japan, including Wakasa, Oki, and Mishima. In the PO dataset analysis, both D_{LK2} and F_{STIS} values reached their maximum at $K = 2$ (Fig. 5E). The Akkeshi sample population was predominant in Cluster 1-1 and the Muroran sample population was predominant in Cluster 1-2 (Fig. 5C).

A consistent genetic population structure was observed for the above cluster analysis and 6 subgroups
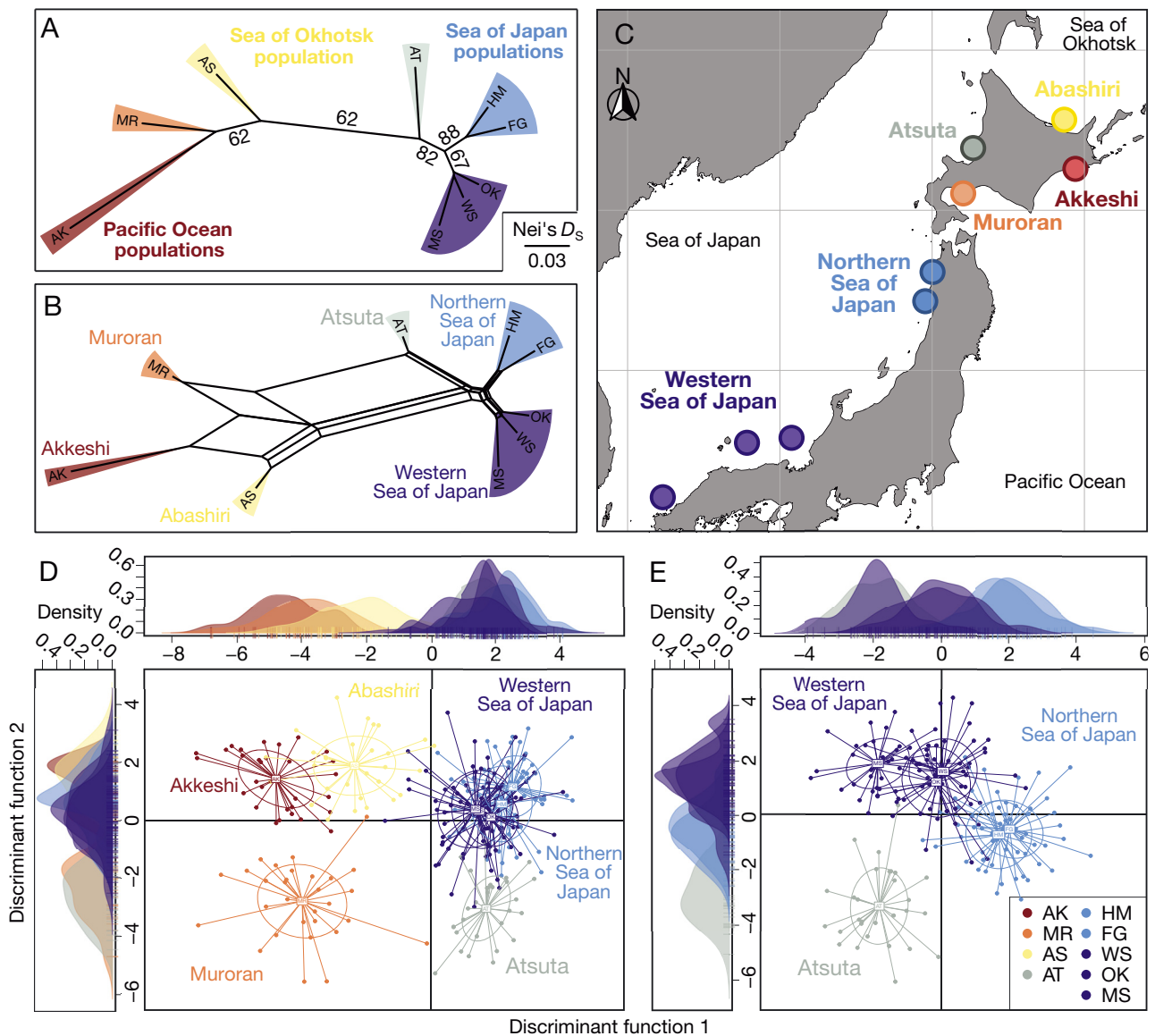
Fig. 4. (A) Neighbor-joining tree and (B) neighbor-net based on Nei's standard genetic distance (D_S) calculated from the 10 microsatellite DNA loci. For branches of neighbor-joining trees that had a bootstrap value greater than 50%, the value is shown in the internal branches. (C) Geographic location of each subgroup. Discriminant analysis of principal components based on (D) all sample populations and (E) the Sea of Japan sample populations. Colors in (C) correspond to those in the other panels, indicating the different subgroups identified. See Table 1 for sample population abbreviations

were identified (Fig. 4C): Akkeshi, Muroran, Abashiri, Atsuta, the Northern Sea of Japan (Hachimori and Funagawa), and the Western Sea of Japan (Wakasa, Oki, and Mishima). The fixation index between subgroups showed statistically significant genetic differentiation in all combinations except for some R_{ST} values (Table 4). The fixation index tended to indicate greater genetic differentiation between subgroups in different sea areas than between subgroups within the same sea area. When the variance components were examined at the sea area level by AMOVA, the variance between subgroups across sea areas ($V_a = 0.139$, p = 0.014) was larger than that within subgroups of the same sea area ($V_b = 0.052$, p < 0.001; Table 5). When the variance components of the detected subgroups were examined by AMOVA, the variance between groups ($V_a = 0.154$, p < 0.001) was significant, while the within-group variance between sample populations ($V_b = -0.005$, p = 0.718) was statistically zero, and no further group structure was supported.
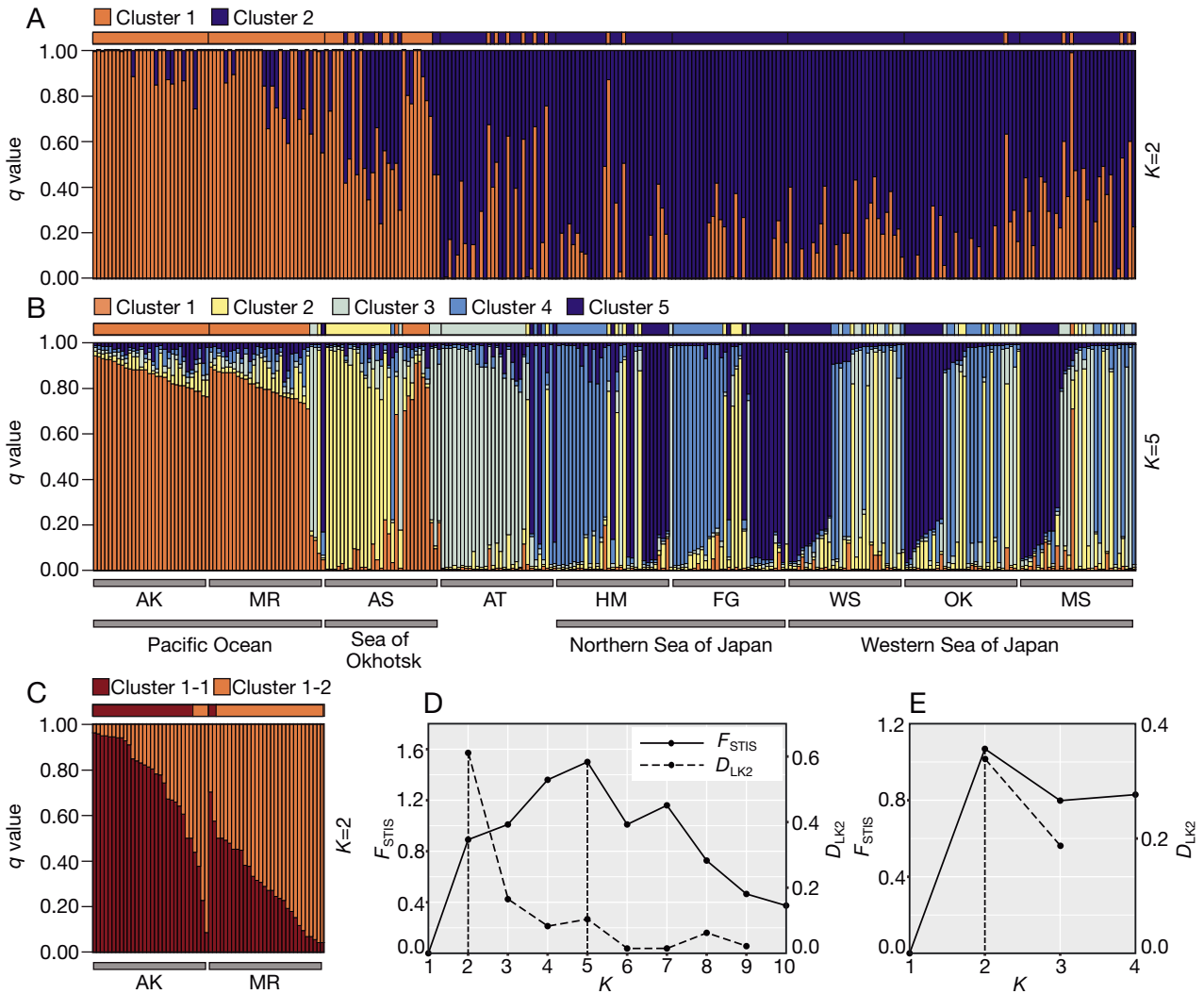
Fig. 5. PopCluster analysis based on the 10 microsatellite loci for (A,B,D) all sample populations and (C,E) the Pacific Ocean sample populations. The assignment probability (q value) of each individual to each cluster based on the admixture model is shown below and the clusters to which each individual was assigned by the k-means method are shown above (A,B,C). The optimal number of clusters K (vertical dotted lines) was suggested by D_{LK2} or (and) F_{STIS} values (D,E). See Table 1 for sample population abbreviations

Table 4. Genetic divergence among the 6 subgroups of *Arctoscopus japonicus* around Japan. Below diagonal: pairwise F_{ST}; above diagonal: pairwise R_{ST}. Statistical significance was tested by permutation tests (10 000 permutations), and p-values (in parentheses) were corrected by sequential Bonferroni. The Northern Sea of Japan includes Hachimori and Funagawa, and the Western Sea of Japan includes Wakasa, Oki, and Mishima samples

Subgroups	Akkeshi	Muroran	Abashiri	Atsuta	Northern Sea of Japan	Western Sea of Japan
Akkeshi		0.03107 (0.048)	0.05542 (0.004)	0.41408 (<0.001)	0.35069 (<0.001)	0.21994 (<0.001)
Muroran	0.02833 (<0.001)		−0.00078 (0.414)	0.31337 (<0.001)	0.28157 (<0.001)	0.15771 (<0.001)
Abashiri	0.02157 (<0.001)	0.02593 (<0.001)		0.23943 (<0.001)	0.21929 (<0.001)	0.10615 (<0.001)
Atsuta	0.07562 (<0.001)	0.04018 (<0.001)	0.05188 (<0.001)		0.00219 (0.681)	0.03474 (0.051)
Northern Sea of Japan	0.05924 (<0.001)	0.05012 (<0.001)	0.03667 (<0.001)	0.02165 (<0.001)		0.03491 (0.010)
Western Sea of Japan	0.06549 (<0.001)	0.05251 (<0.001)	0.03789 (<0.001)	0.02209 (<0.001)	0.00947 (<0.001)	

Table 5. AMOVA based on microsatellite loci. The genetic variance was obtained when dividing the population into 3 groups for the Sea of Japan, the Pacific Ocean, and the Sea of Okhotsk, as well as when dividing the population into 6 subgroups identified through cluster analysis

Hierarchical model	Source of variation	df	Variance components (p-value)	Percentage of variation
Separated sea areas	Among sea areas (V_a)	2	0.1393 (0.014)	3.44
	Within sea areas (V_b)	6	0.0521 (<0.001)	1.29
	Within sample populations (V_c)	531	3.8575 (<0.001)	95.27
Six subgroups	Among subgroups (V_a)	5	0.1514 (<0.001)	3.78
	Within subgroups (V_b)	3	−0.0050 (0.781)	−0.13
	Within sample populations (V_c)	531	3.8575 (<0.001)	96.34

3.3. Demographic history of the groups

Neutrality indices for the WJ group all showed significantly negative values, indicating an expansion of population size in the past (Tajima's D = −2.20, p = 0.002; Fu's F_S = −25.64, p < 0.001). However, although both neutrality indices for the SH group were negative, Tajima's D did not show significance (Tajima's D = −0.71, p = 0.229; Fu's F_S = −24.71, p < 0.001); therefore, only weak support for population expansion was obtained for this group.

The phylogenetic analysis based on mitochondrial genome datasets, a time-calibrated tree of the suborder Cottoidei, was estimated (Fig. S1). The same topology was reconstructed across different datasets and partitioning schemes, confirming that these analysis conditions did not affect the tree topology. The results of each analysis are shown in Table S5. The molecular evolutionary rate of the cyt*b* region estimated from this analysis was 0.0352 changes per site per million years (95% HPD: 0.0184−0.0535; Fig. S2). This molecular evolutionary rate was used in the following analysis.

The possible scenarios were evaluated using ABC. For Scenarios 1, 2, 3, 4, 5, and 6, the posterior probabilities were 0.0000 (95% CI = 0.0000−0.0127), 0.0144 (0.0000−0.0295), 0.0000 (0.0000−0.0120), 0.1909 (0.1403−0.2416), 0.0049 (0.0000−0.0175), and 0.7891 (0.7376−0.8406), respectively (tolerance rate: 0.001), and Scenario 6 had the highest posterior probability. Changing the tolerance rate from 0.001 to 0.01 did not alter the selected scenario, and there was no overlap in the confidence intervals with other scenarios (Fig. 6B). The reliability of this scenario selection was evaluated by predicting the true scenario from simulated data, and the probability of correctly predicting the scenario from simulated data was 80.0% when the true scenario was Scenario 6. However, when the true scenario was Scenario 4, there was only a 68.9% chance of predicting Scenario 6 instead of 4, and it

was difficult to distinguish between these 2 scenarios. Scenario 4 is a special case of Scenario 6 with r = 0 (admixture proportion) and differs in that it does not consider secondary contact between groups during the post-glacial period. In Scenario 6, most of the summary statistics of the simulation data did not deviate significantly from the observed values, which were within the prior distribution in the PCA (Fig. S3). The best scenario, Scenario 6, suggests that the WJ and SH group diverged at time t_2 = 49 250 (95% HPD = 23 300−139 000) yr ago, before the LGM, followed by a population expansion of the WJ group at time t_1 = 13 925 (6175−18 725) yr ago during the post-glacial period, and secondary contact between the SH and WJ groups occurred at time t_0 = 164 (25−5525) yr ago (r = 0.0186, 0.0003−0.2710; Fig. 6A). Other estimated parameters are listed in Table S6.

A skyline plot was constructed using MIGRATE. The fN_e of the SH group remained nearly constant throughout the period, while the N_e of the WJ group increased rapidly from about 20 kya (Fig. 6C). The estimated m value suggests that the forward female migration rate from the WJ group to the SH group has increased since about 25 kya (Fig. 6D).

4. DISCUSSION

4.1. Fine-scale genetic population structure within each sea area

We revealed significant genetic population structure between spawning areas in *Arctoscopus japonicus*. This structure has a hierarchical character. Specifically, analysis of both mtDNA and msDNA indicated significant differentiation between major sea areas (Pacific Ocean, Sea of Japan, and Sea of Okhotsk, V_a; Tables 2 & 5). In addition, *A. japonicus* is differentiated at a fine scale within each sea area, even in continuous habitats without geographic barriers.
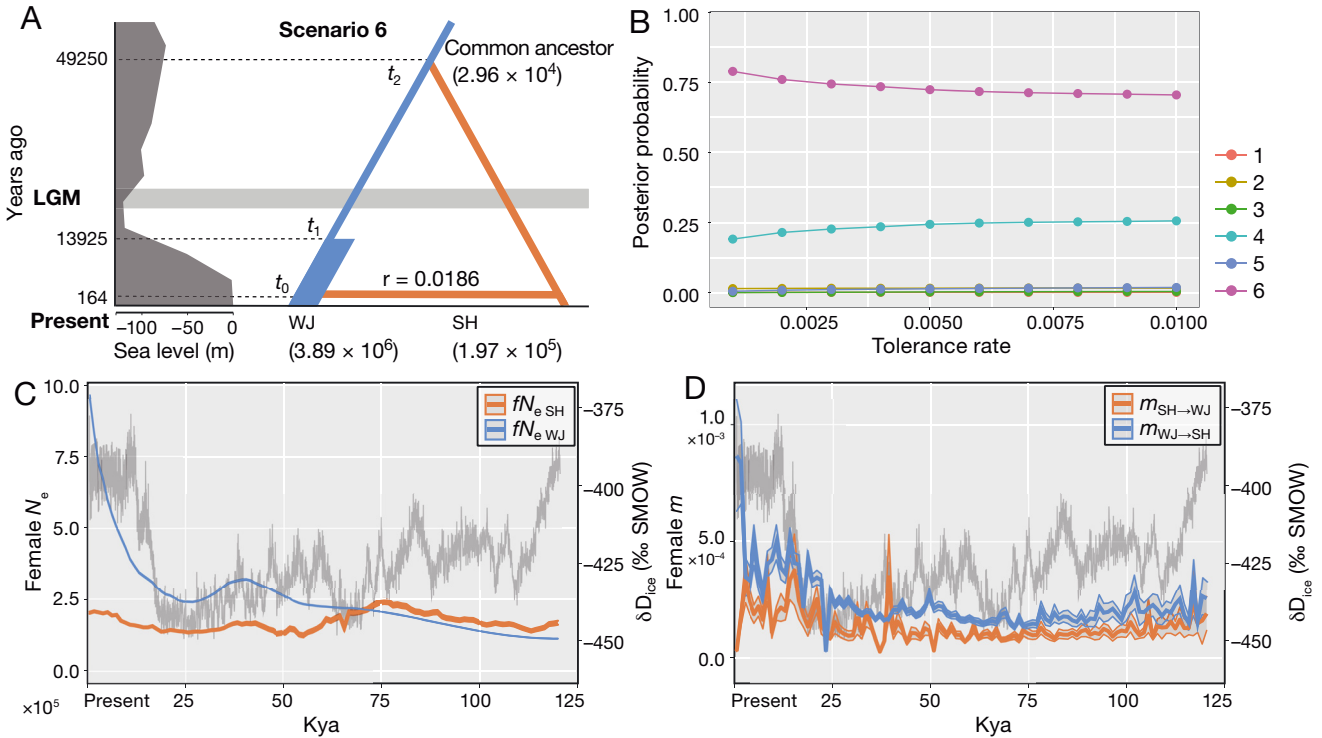
Fig. 6. (A) Estimated parameter values for the best scenario selected by approximate Bayesian computation (ABC). The numbers in parentheses in scenario 6 represent the effective population size. The sea level change (Miller et al. 2005) is shown to the left. LGM: Last Glacial Maximum. (B) Posterior probabilities of each scenario when the tolerance rate of simulated values is changed from 0.001 to 0.01%. Numbers in the key correspond to the scenario numbers in Fig. 2. Transition times for (C) female effective population size (fN_e) and (D) migration rate (m) in the West coast of Japan (WJ) and Southern Hokkaido (SH) populations. The δD value obtained from Antarctic ice core records (Jouzel et al. 2007; grey; SMOW: standard mean ocean water) is correlated with past temperature changes

These results are broadly consistent with those of Shirai et al. (2006). However, our study further elucidates the genetic characteristics of the Sea of Okhotsk population and provides new insights into the fine-scale population structure within each sea area.

4.1.1. Genetic population structure within Pacific Ocean

Concerning the population structure along the Pacific coast of Hokkaido, the PopCluster analysis based on the PO dataset and DAPC revealed that the Akkeshi and the Muroran populations included in the SH group are differentiated genetically and therefore likely to exhibit a level of demographic independence (Figs. 4D & 5C). These populations are independently managed as the Kushiro (Akkeshi) and the Funka Bay (Muroran) stocks (Hoshino 2011), respectively, and exhibit significant differences in morphology (Kobayashi & Kaga 1981), and rate of copepod parasitism (Yanagimoto & Konishi 2004). This difference suggests that the feeding migration areas of the 2 stocks are dif-

ferent. The results presented in the present study support the hypothesis that both stocks are independent populations that are well differentiated both genetically and ecologically. The Pacific coast of Hokkaido, where both populations are distributed, is served by both the Oyashio Current (cold current) and the Tsugaru Warm Current (cf. Fig. 1), resulting in different winter water temperatures between the spawning grounds. This environmental difference may have contributed to the divergence of these 2 populations.

4.1.2. Genetic population structure within the Sea of Japan

With regard to the Sea of Japan, our results indicate there are at least 3 genetically and geographically distinct populations: Atsuta, the Northern Sea of Japan, and the Western Sea of Japan. This adds significant detail to the results presented previously by Shirai et al. (2006) which reported 2 genetic groups: one primarily derived from spawning grounds along the coast of Akita prefecture and Atsuta in Ishikari Bay

(WJ group) and the other mainly from spawning grounds along the eastern coast of the Korean Peninsula (EK group). In the present study, we observed 2 mtDNA cyt*b* lineages corresponding to the haplogroups reported by Shirai et al. (2006): Clades A and C (Fig. 3A), with the same group structure detected by SAMOVA clustering (Table 2). In addition, our analysis based on msDNA variations revealed genetic differences between 2 spawning schools (Atsuta and the Northern Sea of Japan) within the WJ group that could not be detected by mtDNA analysis (Figs. 4 & 5, Table 4). The former corresponds to the stock of Ishikari Bay and the latter to the Northern Sea of Japan.

4.1.3. Correspondence between genetic results and tag release data

According to tagging surveys and fishery records, individuals released in the spawning grounds of Ishikari Bay (Atsuta) tend to be caught in the northern Teuri basin, north of the spawning grounds (Hoshino & Mihashi 2011). In contrast, individuals released in Akita Prefecture (Northern Sea of Japan) tend to be recaptured in southern parts of the spawning grounds, such as off Sado Island and the adjacent coast of Niigata, suggesting they migrate southward from their spawning grounds (Okiyama 1970). Our results are consistent with this; however, the relatively low fixation indices between them suggest that they are not completely independent but are connected through migration.

4.1.4. Genetic characteristics of the Sea of Okhotsk population

The cluster analysis based on msDNA revealed unique genetic characteristics of the previously unexplored Sea of Okhotsk (i.e. Abashiri) population. In the PopCluster analysis assuming $K = 2$, individuals were distinguished as either belonging to the Pacific-type cluster (Cluster 1) or exhibiting an admixed pattern between the Pacific-type and Sea of Japan-type clusters (Clusters 1 and 2). When $K = 5$ was assumed, the admixed individuals were assigned to a unique cluster (Fig. 5). The DAPC analysis indicated that many individuals from this population exhibited genotypes intermediate between those of the Sea of Japan and the Pacific individuals, with some indistinguishable from the Pacific individuals (Fig. 4D). These findings suggests that the Abashiri population comprises hybrid individuals from the

Sea of Japan and the Pacific, as well as migrants from the Pacific.

The morphological study supports these findings. According to the cluster analysis conducted by Kobayashi & Kaga (1981), samples from the Sea of Japan, the Pacific, and the Sea of Okhotsk form distinct morphological clusters, with the Sea of Okhotsk cluster being closer to the Pacific cluster than to the Sea of Japan cluster. These morphological characteristics further support the notion that the Abashiri population consists of individuals with admixed features and migrants from the Pacific.

4.2. Demographic history of the Sea of Japan and Pacific Ocean groups

The results of our analyses based on the mtDNA and msDNA variations have clarified the detailed historical genetic relationship between the Sea of Japan (WJ) and Pacific Ocean (SH) groups, as reported by Shirai et al. (2006). The demographic history of these groups appears to have been influenced by climate change during the Pleistocene. Our analysis suggests that the divergence of these groups can be explained by the fragmentation of regional populations due to changes in connectivity between sea areas caused by sea level decline during the LGM. Furthermore, fluctuations in population size may be related to changes in habitat conditions in each sea area since the last glacial period. In the following sections, we present detailed evidence supporting these conclusions.

4.2.1. Historical relationship between the groups

Through the mtDNA and msDNA variations analyses conducted in the present study, relatively large genetic differences were observed between *A. japonicus* populations in the Sea of Japan and the Pacific Ocean. Different mtDNA clades were dominant in sample populations in their respective locality, and the Φ_{ST} values between local populations across different localities were high (Fig. 3A, Table 3). Additionally, R_{ST} values based on variations showed significant differentiation between local populations across different localities, and it was found that not only allele frequencies but also allele size ranges were different between populations from different groups (Table 4). These findings suggest that since the ancestral populations of the Sea of Japan and the Pacific Ocean diverged, step-wise mutations have

accumulated in their daughter populations, and it is highly likely that they were historically isolated from each other. However, the phylogenetic relationships of mtDNA haplotypes were not reciprocally monophyletic for each locality (Fig. 3A; 'Phylogeographic category II' in Avise 2000). This branching pattern in the gene tree may be caused by incomplete lineage sorting, recent gene flow between the Japan Sea and Pacific populations, or both.

Based on ABC and MIGRATE analysis, it is estimated that the divergence between the WJ (Sea of Japan) and SH (Pacific Ocean) groups in the 2 sea areas occurred at least before the LGM, and that there was secondary contact between them after the postglacial period (Fig. 6A,D, Table S6). During the Quaternary glacial periods, global cooling occurred and polar ice sheets developed, causing a decrease in sea level. Conversely, during warm interglacial periods, sea levels rose, and these sea level fluctuations resulted in repeated transgressions and regressions, changing the connectivity between the sea areas around the Japanese archipelago (Oba et al. 1991, Tada et al. 1999, Itaki et al. 2004; Fig. 1). The Sea of Japan, which is connected to other seas only by shallow straits (about 13 to 130 m depth), is thought to have historically experienced repeated connections and disconnections with the Pacific Ocean and the Sea of Okhotsk (Nishimura 1990). The estimated relationship between the WJ and SH groups could have been caused by the geographic isolation and subsequent reconnection of the 2 sea areas during the glacial period.

The Tsugaru Strait (about 125 to 130 m depth, cf. Yashima & Miyauchi 1990) may be involved in the geographical isolation of the 2 groups, considering the current geographic distribution of this species (Matsubara & Ochiai 1965, Okiyama 1990, Shirai et al. 2007). During the LGM, sea level was 120 to 130 m below present level (Miller et al. 2005, Yokoyama et al. 2018). While the formation of the Tsugaru land bridge is debated (Yashima & Miyauchi 1990), the strait likely narrowed to at least about 2 km wide and 10 m deep during the LGM. For adults of this species, which live at the sea bottom at a temperature of 5°C or lower and 200 to 400 m depths during the migration season, this sea level regression was probably sufficient to limit gene flow between populations in these regions, leading to their divergence. Additionally, secondary contact between the 2 groups after their divergence, around 10 kya, is likely due to post-glacial sea level rise and the subsequent removal of geographical isolation barriers.

4.2.2. Population size history and climate change

Sea level changes during glacial–interglacial cycles not only altered the connectivity between sea areas but also led to subsequent changes in the marine environment within these areas (Nishimura 1990). During the LGM, the cessation of the Tsushima Warm Current led to stratification and oxygen depletion in the deep regions of the Sea of Japan due to the influx of freshwater from the continent (Oba et al. 1991, Tada et al. 1999). In contrast, during the interglacial period, the influx of the Tsushima Warm Current improved the living environment. In particular, it is estimated that the deep anoxic state was rapidly resolved after the LGM, at around 14 kya (Itaki et al. 2004). The population of *A. japonicus* in the Sea of Japan is thought to have repeatedly declined or become locally extinct due to the dramatic environmental changes that occurred during the Pleistocene. The negative Tajima's D and Fu's F_S values, the best scenario selected by ABC, and the skyline plot constructed by MIGRATE support population size expansion of the WJ group and an increase in the migration rate from the WJ to the SH group after the LGM (Fig. 6A). Such contrasting population size histories between the Sea of Japan and other sea areas have been reported not only for this species but also for other deep sea demersal fish (e.g. *Lycodes matsubarai*; Sakuma et al. 2014). This can be interpreted as indicating (1) the isolation of the Sea of Japan population in a refuge during the LGM and (2) an increase in the carrying capacity due to improvement in the living environment after the LGM.

4.3. Implications for conservation and management strategies

The analysis based on microsatellite DNA loci bridged the gap in the understanding of the population structure of *A. japonicus* between previous morphometric and genetic studies. Each spawning school appears to have a unique migration range, with limited migration of individuals between spawning schools. This finding is crucial for maintaining the genetic diversity of regional populations and ensuring the future adaptive potential of the species (Moritz 1994, Palsbøll et al. 2007). From this perspective, the current resource management strategy, which has set conservation management units for each spawning school and focused conservation efforts accordingly, is considered appropriate.

The Sea of Japan and Pacific Ocean groups of this species have historically distinct evolutionary demo-

graphy. Gene flow between these groups is likely to have occurred after the geographic barriers were removed at the end of the LGM. Whether these groups will eventually fuse or maintain their distinct lineages despite the presence of gene flow depends significantly on whether they have undergone local adaptation to their respective environments.

On the other hand, in the present study, we were unable to elucidate the evolutionary background behind the formation of the Sea of Okhotsk population. This limitation is due to the limitations of the genetic markers used, which are not suitable for analyzing population demography involving hybridization. Specifically, while mtDNA sequence data provide genealogical information, these sequences are maternally inherited and unsuitable for analyzing population demography involving hybridization and high-level geneflow. In contrast, msDNA data are well-suited to detecting hybridization, but are challenging to use for estimating historical demography due to the high evolutionary rates and complex mutational processes (Morin et al. 2004). The historical background of the Sea of Okhotsk population, as well as the degree of local adaptation to the respective environments in each population, are expected to be clarified by future population genomic analyses based on genome-wide SNPs.

Regarding this species, artificial seed has been produced in the past to enhance natural resources (Sugiyama & Morioka 2002). If such projects are resumed in the future, to avoid the risk of reducing adaptive potential due to genetic disruption, it would be ideal for the release sites of juveniles to match, at minimum, the capture locations of the parent at the spawning school (population) level, and preferably at the sea area (genetic group) level.

5. CONCLUSIONS

Our analyses of mtDNA and msDNA have revealed that *Arctoscopus japonicus* is composed of at least 6 genetically differentiated populations with a hierarchical structure. The genetic groups differentiated in the Sea of Japan and the Pacific Ocean are likely to have been influenced by changes in coastal topography and marine environments associated with sea level fluctuations since the last glacial period. The population in the Sea of Okhotsk, investigated for the first time in this study, possesses distinctive genetic characteristics, suggesting that hybridization between populations from the Sea of Japan and the Pacific Ocean may have played a role in its formation. These findings provide important information not only for

formulating resource management strategies for this species, but also for understanding the natural history of marine fishes inhabiting the seas around Japan.

LITERATURE CITED

Avise JC (2000) Phylogeography: the history and formation of species. Harvard University Press, Cambridge

Beerli P (2006) Comparison of Bayesian and maximum-likelihood inference of population genetic parameters. Bioinformatics 22:341—345

Blacket MJ, Robin C, Good RT, Lee SF, Miller AD (2012) Universal primers for florescent labelling of PCR fragments — an efficient and cost-effective approach to genotyping by florescence. Mol Ecol Resour 12:456—463

Bouckaert R, Heled J, Kühnert D, Vaughan T and others (2014) BEAST 2: a software platform for Bayesian evolutionary analysis. PLOS Comput Biol 10:e1003537

Bryant D, Moulton V (2004) Neighbor-Net: an agglomerative method for the construction of phylogenetic networks. Mol Biol Evol 21:255—265

Cornuet JM, Pudlo P, Veyssier J, Dehne-Garcia A and others (2014) DIYABC v2.0: a software to make approximate Bayesian computation inferences about population history using single nucleotide polymorphism, DNA sequence and microsatellite data. Bioinformatics 30:1187—1189

dos Reis M, Yang Z (2011) Approximate likelihood calculation on a phylogeny for Bayesian estimation of divergence times. Mol Biol Evol 28:2161—2172

Dupanloup I, Schneider S, Excoffier L (2002) A simulated annealing approach to define the genetic structure of populations. Mol Ecol 11:2571—2581

Excoffier L, Lischer HEL (2010) Arlequin suite ver 3.5: a new series of programs to perform population genetics analyses under Linux and Windows. Mol Ecol Resour 10:564—567

Felsenstein J (1981) Evolutionary trees from DNA sequences: a maximum likelihood approach. J Mol Evol 17:368—376

Fu YX (1997) Statistical tests of neutrality of mutations against population growth, hitchhiking and background selection. Genetics 147:915—925

Fujino K, Amita Y (1984) Subpopulation identification of the sailfin sandfish from waters adjacent to Japan. Fish Genet Breed Sci 9:31–39 (in Japanese)

Fujiwara K, Yagi Y, Yoshikawa A, Sakuma K, Iida M, Shirakawa H, Yamamoto T (2020) Stock assessment and evaluation for Western Sea of Japan stock of the sailfin sandfish (fiscal year 2020). https://abchan.fra.go.jp/wpt/wp-content/uploads/2020/details_2020_52.pdf (accessed 7 June 2023) (in Japanese)

Guichoux E, Lagache L, Wagner S, Chaumeil P and others (2011) Current trends in microsatellite genotyping. Mol Ecol Resour 11:591–611

Hasegawa M, Kishino H, Yano T (1985) Dating of the human–ape splitting by a molecular clock of mitochondrial DNA. J Mol Evol 22:160–174

Hoshino N (2011) I. Biological and ecological characteristics of the sailfin sandfish. In: Hokkaido Research Organization Fisheries Research Department (ed) Stocks of sailfin sandfish (Arctoscopus japonicus) in the waters around Hokkaido. Technical Report No. 7. HRO, Yoichi, p 1–16 (in Japanese)

Hoshino N, Mihashi M (2011) II-1. Ishikari stock. In: Hokkaido Research Organization Fisheries Research Department (ed) Stocks of sailfin sandfish (Arctoscopus japonicus) in the waters around Hokkaido. Technical Report No. 7. HRO, Yoichi, p 17–32 (in Japanese)

Hotaling S, Muhlfeld CC, Giersch JJ, Ali OA and others (2018) Demographic modelling reveals a history of divergence with gene flow for a glacially tied stonefly in a changing post-Pleistocene landscape. J Biogeogr 45:304–317

Huson DH, Bryant D (2006) Application of phylogenetic networks in evolutionary studies. Mol Biol Evol 23:254–267

Iida M, Fujiwara K, Yagi Y, Shirakawa H (2020) Stock assessment and evaluation for Western Sea of Japan stock of the sailfin sandfish (fiscal year 2020). https://abchan.fra.go.jp/wpt/wp-content/uploads/2020/details_2020_53.pdf (accessed 7 June 2023) (in Japanese)

Imamura H, Shirai SM, Yabe M (2005) Phylogenetic position of the family Trichodontidae (Teleostei: Perciformes), with a revised classification of the perciform suborder Cottoidei. Ichthyol Res 52:264–274

Inoue J, Donoghue PCJ, Yang Z (2010) The impact of the representation of fossil calibration on Bayesian estimation of species divergence times. Syst Biol 59:74–89

Itaki T, Ikehara K, Motoyama I, Hasegawa S (2004) Abrupt ventilation changes in the Japan Sea over the last 30 ky: evidence from deep-dwelling radiolarians. Palaeogeogr Palaeoclimatol Palaeoecol 208:263–278

Jombart T, Devillard S, Balloux F (2010) Discriminant analysis of principal components: a new method for the analysis of genetically structured populations. BMC Genet 11:94

Jouzel J, Masson-Delmotte V, Cattani O, Dreyfus G and others (2007) Orbital and millennial Antarctic climate variability over the past 800,000 years. Science 317:793–796

Katoh K, Standley DM (2013) MAFFT multiple sequence alignment software version 7: improvements in performance and usability. Mol Biol Evol 30:772–780

Kimura M, Crow JF (1964) The number of alleles that can be maintained in a finite population. Genetics 49:725–738

Kiyokawa T (1991) Distribution and migration of the sandfish (Arctoscopus japonicus) in the western part of the Japan Sea. Contrib Fish Res Japan Sea Block 21:51–66 (in Japanese)

Kobayashi T, Kaga Y (1981) Population of sandfish, Arctoscopus japonicus (Steindachner), in the seas around Hokkaido estimated from the variations of meristic characters. Bull Hokkaido Reg Fish Res Lab 46:69–83 (in Japanese with English Abstract)

Kück P, Meusemann K (2010) FASconCAT: convenient handling of data matrices. Mol Phylogenet Evol 56:1115–1118

Kumar S, Stecher G, Tamura K (2016) MEGA7: molecular evolutionary genetics analysis version 7.0 for bigger datasets. Mol Biol Evol 33:1870–1874

Kurihara H, Ikeda M (2022) Screening of microsatellite DNA markers for population genetic analysis of sailfin sandfish Arctoscopus japonicus. Aquat Anim 2022:AA2022-14 (in Japanese with English Abstract)

Matsubara K, Ochiai A (1965) Ichthyology, Vol 2. Koseisha-Koseikaku, Tokyo

Mecklenburg CW (2003) Family Trichodontidae Bleeker 1859 — sandfishes. Calif Acad Sci Annotated Checklists of Fishes No. 15. California Academy of Sciences, San Francisco, CA

Miller KG, Kominz MA, Browning JV, Wright JD and others (2005) The Phanerozoic record of global sea-level change. Science 310:1293–1298

Miya M, Nishida M (2000) Use of mitogenomic information in teleostean molecular phylogenetics: a tree-based exploration under the maximum-parsimony optimality criterion. Mol Phylogenet Evol 17:437–455

Morin PA, Luikart G, Wayne RK, SNP workshop group (2004) SNPs in ecology, evolution and conservation. Trends Ecol Evol 19:208–216

Moritz C (1994) Defining 'evolutionarily significant units' for conservation. Trends Ecol Evol 9:373–375

Nei M (1972) Genetic distance between populations. Am Nat 106:283–291

Nelson JS, Grande TC, Wilson MV (2016) Fishes of the world, 5th edn. John Wiley & Sons, Hoboken, NJ

Nishimura S (1990) Origin and history of the Sea of Japan: an approach from the biogeography, 3rd edn. Tsukiji Shobo, Tokyo (in Japanese)

Oba T, Kato M, Kitazato H, Koizumi I, Omura A, Sakai T, Takayama T (1991) Paleoenvironmental changes in the Japan Sea during the last 85,000 years. Paleoceanography 6:499–518

Okiyama M (1970) Studies on the population biology of the sand fish, Arctoscopus japonicus (Steindachner). II. Population analysis (preliminary report). Nihonkai-ku Suisan Kenkyujo Kenkyu Hokoku 22:59–69 (in Japanese with English Abstract)

Okiyama M (1990) Contrast in reproductive style between two species of sandfishes (family Trichodontidae). Fish Bull 88:543–549

Palsbøll PJ, Bérubé M, Allendorf F (2007) Identification of management units using population genetic data. Trends Ecol Evol 22:11–16

Peakall R, Smouse PE (2012) GenAlEx 6.5: genetic analysis in Excel. Population genetic software for teaching and research — an update. Bioinformatics 28:2537–2539

Rambaut A, Drummond AJ, Xie D, Baele G, Suchard MA (2018) Posterior summarization in Bayesian phylogenetics using Tracer 1.7. Syst Biol 67:901–904

Rice WR (1989) Analyzing tables of statistical tests. Evolution 43:223–225

Saitou N, Nei M (1987) The neighbor-joining method: a new method for reconstructing phylogenetic trees. Mol Biol Evol 4:406–425

Sakuma K, Ueda Y, Hamatsu T, Kojima S (2014) Contrasting population histories of the deep-sea demersal fish, *Lycodes matsubarai*, in the Sea of Japan and the Sea of Okhotsk. Zoolog Sci 31:375−382

Shirai SM, Kuranaga R, Sugiyama H, Higuchi M (2006) Population structure of the sailfin sandfish, *Arctoscopus japonicus* (Trichodontidae), in the Sea of Japan. Ichthyol Res 53:357−368

Shirai SM, Goto T, Hirose T (2007) Sail-fin sandfish (*Arctoscopus japonicus*) collected off the Iwate area in February to March, 2004: evidence that they came from the Sea of Japan. Jpn J Ichthyol 54:47−58 (in Japanese with English Abstract)

Stamatakis A (2014) RAxML version 8: a tool for phylogenetic analysis and post-analysis of large phylogenies. Bioinformatics 30:1312−1313

Sugiyama H, Morioka T (2002) I. Efforts and history of increasing of the sailfin sandfish resources. In: Sugiyama H, Morioka T, Konaga H, Sugishita S, Nagakura Y (eds) The biological characteristics and seed production technology of the sailfin sandfish. Aquaculture Technology Series No. 8. Japan Sea-Farming Association, Tokyo, p 1−6

Tada R, Irino T, Koizumi I (1999) Land-ocean linkages over orbital and millennial timescales recorded in late Quaternary sediments of the Japan Sea. Paleoceanography 14:236−247

Tajima F (1989) Statistical method for testing the neutral mutation hypothesis by DNA polymorphism. Genetics 123:585−595

Tamura K, Nei M (1993) Estimation of the number of nucleotide substitutions in the control region of mitochondrial DNA in humans and chimpanzees. Mol Biol Evol 10:512−526

Wang J (2022) Fast and accurate population admixture inference from genotype data from a few microsatellites to millions of SNPs. Heredity 129:79−92

Yanagimoto T (2004) Geographic population subdivision of the Japanese sandfish, *Arctoscopus japonicus*, inferred from PCR-RFLP analysis on mtDNA. Nippon Suisan Gakkaishi 70:583−591 (in Japanese with English Abstract)

Yanagimoto T, Konishi K (2004) *Acanthochondria priacanthi* (Copepoda: Chondracanthidae) as a biological indicator for stock identification of sandfish *Arctoscopus japonicus* (Steindachner). Fish Sci 70:336−338

Yang Z (1994) Estimating the pattern of nucleotide substitution. J Mol Evol 39:105−111

Yang Z (2007) PAML 4: phylogenetic analysis by maximum likelihood. Mol Biol Evol 24:1586−1591

Yashima K, Miyauchi T (1990) The Tsugaru land bridge problem related to Quaternary coastal tectonics, northeast Japan. Daiyonki-Kenkyu 29:267−275 (in Japanese with English Abstract)

Yokoyama Y, Esat TM, Thompson WG, Thomas AL and others (2018) Rapid glaciation and a two-step sea level plunge into the Last Glacial Maximum. Nature 559:603−607

Zardoya R, Meyer A (1996) Phylogenetic performance of mitochondrial protein-coding genes in resolving relationships among vertebrates. Mol Biol Evol 13:933−942